Pertanika J. Sci. & Technol. 26 (1): 193 - 214 (2018)

PERTANIKA JOURNALS

SCIENCE & TECHNOLOGY

Journal homepage: http://www.pertanika.upm.edu.my/

High Intrinsic Biosorption Efficiency of Cattle Manure on Cr(VI): A Potential Low-cost Fibre-rich Biosorbent

Yap, K. L.[1], Lee, C. M.[1], Gan, Y. L.[2], Tang, T. K.[1], Lee, Y. Y.[1], Tee, T. P.[3] and Lai, O. M.[1,2]*

[1]Bioprocess Laboratory, Institute of Bioscience, Universiti Putra Malaysia, 43400 UPM, Serdang, Selangor, Malaysia
[2]Department of Bioprocess Technology, Faculty of Biotechnology and Biomolecular Sciences, Universiti Putra Malaysia, 43400 UPM, Serdang, Selangor, Malaysia
[3]Department of Animal Science, Faculty of Agriculture, Universiti Putra Malaysia, 43400 UPM, Serdang, Selangor, Malaysia

ABSTRACT

Fibre-rich manure derived from grass-fed cattle showed significantly higher intrinsic sorption efficiency on Cr(VI) solution as compared to corncob, sawdust and cogon grass. This observation could be attributed to the ligneous nature and rough surface morphology of the cattle manure. Four-factor, three-level, face-centred composite design (FCCD) suggested the process was greatly affected by initial pH of the solution, contact time and sorbent dosage ($p<0.0001$), while stirring rate had negligible effect. Highest percentage removal (≥70%) happened at pH 1-1.56, 0.79-1 g sorbent and 57-300 min contact time in 200 mg/L Cr(VI) solution. The process is spontaneous, endothermic and best described by pseudo-second-order and Langmuir model. It was found that adsorbed Cr(VI) could be recovered and CM could be reused at least three times with >50% adsorption efficiency. It is predicted that both physisorption and chemisorption are involved in the sorption process.

Keywords: Biosorption, cattle manure, chromium (VI), heavy metals, response surface methodology

ARTICLE INFO

Article history:
Received: 16 November 2016
Accepted: 02 June 2017

E-mail addresses:
ykling1990@gmail.com (Yap, K. L.),
choonminlee2010@gmail.com (Lee, C. M.),
yeelingan@gmail.com (Gan, Y. L.),
teckkim1@gmail.com (Tang, T. K.),
leeying911@gmail.com (Lee, Y. Y.),
ttpoy@yahoo.com (Tee, T. P.),
omlai@upm.edu.my; omlai.biotech@gmail.com (Lai, O. M.)
*Corresponding Author

ISSN: 0128-7680

INTRODUCTION

Heavy metal (HM) pollution has long been a serious environmental issue due to its perniciousness even at trace concentration. Non-biodegradability allows HMs to bio-accumulate and bio-magnify along the food chain; this worsens an already alarming situation. Discharge of untreated industrial effluent is the root cause, especially in

developing countries where more than 70% of industrial effluent is discharged without prior treatment (Water, 2009). Hexavalent chromium, Cr(VI), is a harmful HM categorised as a group 1 human carcinogen (IARC, 2012) as it is known to cause various cancers. Cr(VI) is commonly found in wastewater due to its high water solubility, which facilitates the release of toxicity into the environment.

Conventional methods such as chemical precipitation, membrane filtration, electrodialysis, ion exchange and adsorption perform at a comparable level of efficiency and thus, cost plays a decisive role in removing heavy metals from the surrounding environment. The sorption method (ion exchange and adsorption) is preferred due to its relatively cheaper cost (up to 200 USD/million litres) compared to other methods, which can cost up to 500 USD/million litres (Barakat, 2011; Fu & Wang, 2011; Gupta et al., 2012). Although the sorption method is more economical, the synthetic resin and activated carbon used in this method are still a heavy burden for industry to bear.

Agricultural waste (AW) with high lignocellulosic content possesses potential as a cost-effective alternative to replace commercial products. Various surface functional groups contributed by lignocellulose and some proteins of AW make AW suitable for removing divalent HMs (Bailey et al., 1999; Garg et al., 2008). Furthermore, the threatening environmental and disposal issues emerging from the overproduction of AW further intensify the value-added initiative, which is an ideal solution to achieve zero-waste.

Numerous studies on various types of AW have been carried out as stated in the review paper of Ngah and Hanafiah (2008). Miretzky and Cirelli (2010) focussed on the list of AW that were tested to remove Cr. Sawdust, corn waste, leaves, weeds, barks, bagasse and husk were some types of AW that have been studied. Animal waste, a subgroup of AW, is seldom used to remove Cr although it has been shown to have high sorption efficiency for other divalent HMs. Fresh manure excreted from different animals such as turkey (Lima & Marshall, 2005b), sheep (Al-Rub et al., 2002), poultry (Lima & Marshall, 2005a), broiler (Uchimiya et al., 2010), and swine (Meng et al., 2014) showed positive results. Similar studies have also been carried out on cattle-manure compost and cattle-manure vermicompost (Jordão et al., 2010; Jordão et al., 2011; Zaini et al., 2009). Fresh cattle manure (CM), however, has received less attention. It is estimated that there are 1.47 billion head of cattle throughout the world (FAOSTAT, 2013). According to Hofmann and Beaulieu (2006), cattle with an average weight of 635 kg can produce 14 tons of CM annually. Since CM is in abundance and it has higher fibre content over poultry and swine manure due to its feed intake (Chen et al., 2003), it has greater potential to be a cost-effective biosorbent.

The aim of this study was to investigate the feasibility of using native CM excreted from grass-fed cattle to remove Cr(VI). The efficiency was compared with other previously studied lignocellulose materials, namely corncob (C), sawdust (S) and cogon grass (CG) in their native form without structural modification through physical or chemical treatment. The response surface methodology (RSM) was employed to optimise and investigate the single and interactive effect of the important process variables, namely, initial solution pH, contact time (CT), stirring rate (SR) and sorbent dosage (SD) on the sorption process. In addition, the sorption process was examined through kinetic, isotherm and thermodynamic studies.

METHODOLOGY

Materials

Potassium dichromate ($K_2Cr_2O_7$), sodium chloride (NaCl) and nitric acid (HNO_3) were purchased from Fisher Scientific, USA. Sodium hydroxide (NaOH) and hydrochloric acid (HCl) were purchased from Merck Millipore, USA. All the chemicals were of analytical reagent grade except for the HNO_3 which was classified as trace metal grade.

Biosorbent Preparation

Corncob (C) was collected from the local corn industry; hardwood S was purchased from Northeastern Products Corp., NY, USA; CG was collected from a wild grass lawn around Selangor, Malaysia. Fresh CM excreted from grass-fed cattle was collected from the animal farm in Universiti Putra Malaysia. All AW was cleaned and washed with distilled water until no visible surface particulates were observed. Then, they were dried in a hot air oven at 70°C for 1 hour to kill pathogens followed by 60°C for 24 h. The AW was ground using a blender and sieved to particle size of ≤250 µm and stored in an air-tight container for further use. Physicochemical properties of AW are shown in Table 1. Moisture content, total solid, volatile solid and ash content were determined using the EPA method (EPA, 2001). Total carbon and nitrogen were analysed using the CNS TruMac analyser (LECO, USA). Cellulose, hemicellulose and lignin content were determined upon neutral detergent fibre, acid detergent fibre and acid detergent lignin analysis. Total surface negative charge was determined using the modified Boehm (1966) method described in Lima and Marshall (2005b). Point of zero charge was determined using the pH drift method as described in Zaini et al. (2009). The surface morphology before and after sorption experiment (Figure 1[a]-[h]) was observed using scanning electronic microscope (JSM-6400, JOEL, Japan).

Metal Solution Preparation

A Cr(VI) stock solution of 1000 mg/L was prepared by dissolving 2.282 g of $K_2Cr_2O_7$ metal salt in 200 mL of ultrapure (Type 1) water (18.2 MΩ at 25°C) and brought up to 1000 mL with ultrapure (Type 1) water. Working Cr(VI) solutions with different initial metal concentrations (MC) were freshly prepared by diluting the stock accordingly before use.

Table 1
The characteristics of C, S, CG and CM

Parameters	Value			
	C	S	CG	CM
Moisture content (% wet weight)	11.76	9.62	64.20	76.79
Total solid content (TS, % wet weight)	88.24	90.38	35.80	23.21
Volatile solid content (VS, % dry weight)	98.38	99.06	93.79	80.89
Ash content (% dry weight)	1.62	0.94	6.21	19.11
Total negative charge (mmol H+/g)	1.50	1.50	2.70	3.70

Table 1 *(continue)*

pH_{pzc}	4.10	6.80	6.80	7.30
Bulk density (g/cm^3)	0.20	0.26	0.33	0.38
Total carbon (TC, % dry weight)	31.20	33.20	30.10	25.22
Total nitrogen (TN, % dry weight)	0.45	0.01	0.51	1.13
Neutral detergent fibre (NDF, % dry weight)	67.28	76.61	69.28	74.63
Acid detergent fibre (ADF, % dry weight)	31.36	57.54	38.55	54.40
Acid detergent lignin (ADL, % dry weight)	4.13	11.15	4.41	22.15
Cellulose content (% dry weight)	27.23	46.39	34.14	32.25
Hemicellulose content (% dry weight)	35.92	19.07	30.73	20.23

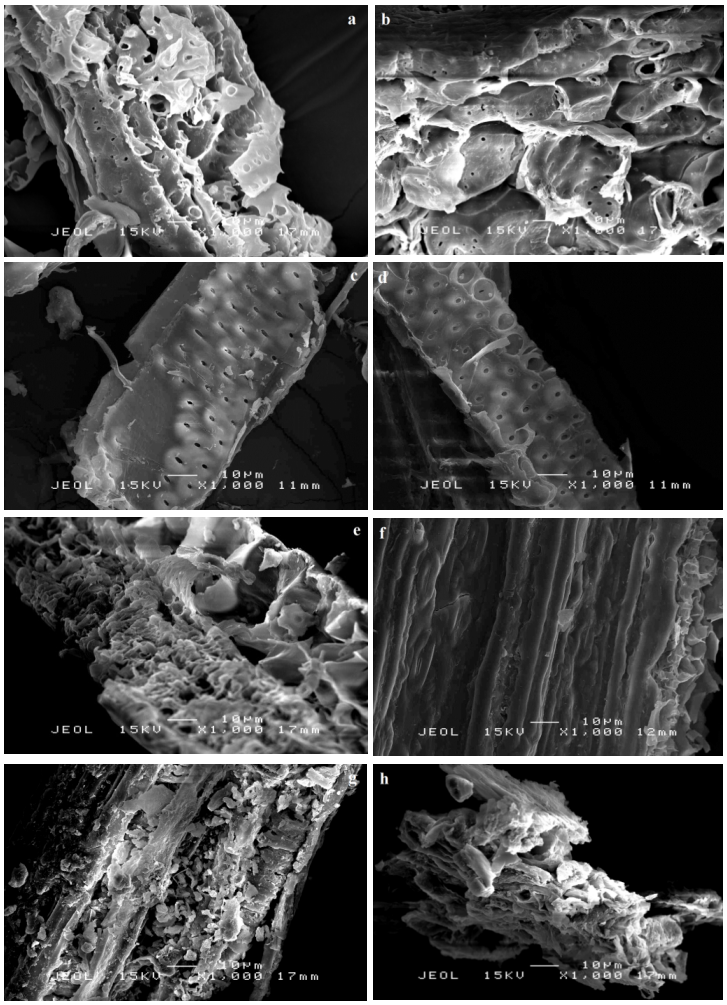

Figure 1. SEM image of (a) C before sorption, (b) C after sorption, (c) S before sorption, (d) S after sorption, (e) CG before sorption, (f) CG after sorption, (g) CM before sorption, (h) CM after sorption (× 1000)

Batch Biosorption Studies

Biosorption efficiency of C, S, CG and CM on Cr(VI) was carried out (i) in low (20 mg/L) and high (200 mg/L) concentrations of Cr(VI) solution at pH 4 (ii) at pH 2 and pH 4 in 200 mg/L Cr(VI) solution. The MC of 200 mg/L was employed because it is the upper limit of the majority of real-life conditions (Masood & Malik, 2011; Shazili et al., 2006). Biosorption was also carried out at 10 times lower MC (20 mg/L) to investigate the performance variation of biosorbents in low MC. Both pH 2 and pH 4 were selected as the initial pH of the solution because the pH of the effluents from the two major contributors of Cr(VI) i.e.: electroplating and tannery industries range from pH 2.2-pH 4.2 (Chowdhury et al., 2015; Vikramjit et al., 2016). Both MC and solution pH were set close to real-life conditions to ensure a practical and applicable biosorbent was identified from this study. Five hundred milligram of biosorbent in 50 mL of metal solution was allowed to equilibrate at 25±2°C for 24 h in both (i) and (ii). Control experiments were carried out without sorbents, and were taken as initial MC. The biosorption process of CM was further investigated in subsequent analysis. A kinetic experiment was performed in 200 mg/L Cr(VI) solution at 25±2°C with CT of 15-1440 min. Sorption isotherm and thermodynamic studies were carried out in MC range of 20-300 mg/L at 25±2°C, 35±2°C and 45±2°C with an equilibrium time of 480 min. The pH was adjusted using 0.1 M HNO3 and 0.5 M NaOH, and measured using a pH meter (Mettler Toledo Ross FE20, USA). The mixture was stirred at 350 r/min using a Teflon-coated magnetic stir bar on a stirring hotplate (Fisher Scientific, USA). It was then filtered through a 0.22 µm PVDF filter (JET BiofilFPV-213-000, China) with the aid of a vacuum pump (Rocker 300, Rocker Scientific Co. Ltd.). The final Cr(VI) concentration after sorption was analysed by ICP-OES (Perkin Elmer Optima 8300). The percentage removal and uptake of Cr(VI) was calculated using Equation [1] and Equation [2]. Graphs were drawn and analysis was done using GraphPad Prism Version 5.02.

$$Percentage\ removal\ (\%) = \frac{(C_0 - C_e)}{C_0} \times 100 \quad [1]$$

$$Uptake, q_e(mg/g) = \frac{(C_0 - C_e) \times V}{m} \quad [2]$$

where C_0 and C_e are the initial and final MC (mg/L), respectively, V is the volume of the metal solution (mL) and m is the amount of biosorbent used (g).

RSM Experimental Design

Biosorption of Cr(VI) by CM was optimised by the four-factor and three-level face-centred central composite design (FCCD) generated using Design Expert 7.0.0 software. The independent variables concerned were the initial pH of the metal solution (x_1, pH), CT (x_2, min), SR (x_3, r/min) and SD (x_4, g). A set of 30 experimental runs with 16 factorial points, eight axial points, and six replicates at the centre point was produced in the FCCD. Experimental runs were conducted randomly in batch mode at room temperature (RT) (25±2°C) in 200 mg/L Cr(VI) solution. The coded and actual values, as well as the range of the independent variables are shown in Table 2. The dependent variable i.e. the percentage removal (%) of Cr(VI) was related to independent parameters through a quadratic polynomial generated from regression analysis.

The generalised quadratic polynomial is shown in Equation [3]:

$$Y = \beta_0 + \sum_{i=1}^{k} \beta_i x_i + \sum_{i=1}^{k} \beta_{ii} x_i^2 + \sum_{i}^{k-1} \sum_{j=i+1}^{k} \beta_{ij} x_i x_j \quad [3]$$

where Y is the dependent response (percentage removal of Cr(VI)), β_0 is the intercept, β_i, β_{ii}, β_{ij} are linear, quadratic and interaction coefficients, respectively; x_i and xj are independent variables in actual unit and k is the number of tested independent variables.

Table 2
The coded and actual values of independent variables

Independent Variables	Unit	Symbol	Range and Level (Coded)		
			-1	0	+1
pH	pH	x_1	1	3	5
Contact time	min	x_2	15	157.5	300
Stirring rate	r/min	x_3	60	205	350
Biosorbent dosage	g	x_4	0.1	0.55	1.0

Desorption and Regeneration

Cattle manure (CM) (0.5 g) was allowed to equilibrate in 50 mL of 200 mg/L metal solution at 25±2°C, pH 2 and 350 r/min for 24 h. The sorbent was then recovered and immersed in 50 mL desorbing agent (0.1 M NaOH) for 30 min, 5 h and 24 h at 25±2°C. The adsorption-desorption cycle was repeated three times to test the regenerability of the sorbent. Desorption efficiency was calculated using Equation 4.

$$\% \text{ desorption} = \frac{C_d}{C_0 - C_e} \times 100 \quad [4]$$

where C_0, C_e and C_d are the initial, equilibrium and desorbed MC (mg/L), respectively.

Quality Assurance

All glassware and plasticware were soaked in 2% HNO_3 overnight and rinsed five times with ultrapure water before use to prevent the contamination of metal ions present in the environment.

RESULTS AND DISCUSSION

Biosorption Efficiency of Biosorbents

The intrinsic biosorption efficiency of C, S, CG and CM in both low (20 mg/L) and high (200 mg/L) Cr(VI) solutions is shown in Figure 2. The sorbents did not undergo surface chemistry and structural modification by either thermochemical (pyrolysis) or chemical pre-treatment. The experimental conditions for the biosorption efficiency tests of the sorbents was kept the same to ensure a fair comparison of the results. At pH 4, higher biosorption was observed in 20 mg/L Cr(VI) solution for all sorbents tested (22.89% for C, 32.50% for S, 54.09% for

CG and 72.53% for CM). As the sorbents' binding sites to metal ions ratio is higher, lower competition increases the chance of Cr(VI) adhering to the binding sites. Biosorption of 200 mg/L Cr(VI) at pH 4 was extremely low for all the sorbents tested (9.49% for C, 14.08% for S, 18.25% for CG and 26.23% for CM), while increased sorption was observed when the pH decreased to pH 2 (35.94% for C, 35.64% for S, 38.37% for CG and 58.68% for CM). In acidic conditions, Cr(VI) exists as $Cr_2O_7^{2-}$ and $HCrO_4^-$ anionic form, and surface protonation occurs when pH of the solution is less than pH_{pzc}; thus, higher sorption was observed at pH 2. Biosorption of CM was significantly higher than C, S and CG, while C exhibited the lowest biosorption performance in both low and high MC and initial pH. Distinctive sorption efficiency may be related to physicochemical characteristics and surface morphology of the sorbents. Although the indigestible fibre content for all types of AW is high (NDF>67% dry weight), their lignocellulose components are different (Table 1). Hemicellulose is the major fibre component of C, while cellulose is the major component in S and CM. CG is composed of almost equal amounts of cellulose and hemicellulose. CM consists of the highest amount of lignin, double the amount of lignin in S and five times those in CG and C. High lignin content in CM could be due to the concentration of lignin after the digestion of cellulose and hemicellulose in the rumen of cattle (Harman et al., 2007). Lignin is an extensively-branched polyphenolic polymer composed of various functional groups responsible for the sorption of Cr(VI) such as hydroxyl, carbonyl and carboxyl groups. Dupont et al. (2004) demonstrated that Cr preferably adhered to microstructures rich in lignin.

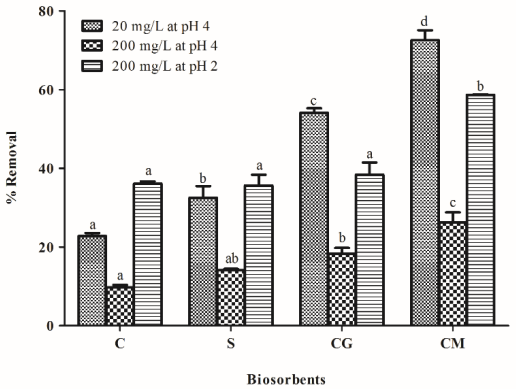

Figure 2. Biosorption efficiency of C, S, CG and CM in 20 mg/L Cr(VI) solution at pH 4 and 200 mg/L Cr(VI) solution at pH 2 and 4 (SD: 0.5 g, SR: 350 r/min, temperature: 25°C, CT: 24 h). Different letters indicate significant difference ($p<0.05$) between sorbents in the same MC and initial pH. Values are mean ± SD (n=3)

A similar finding was reported whereby lignin played a significant role in the biosorption of Cr, but no appreciable sorption was observed in pure cellulose (Dupont & Guillon, 2003). The study claimed that lignin acts as an electron donor and reduces Cr(VI) to Cr(III) in acidic conditions, while oxidation of lignin results in the increase of hydroxyl and carboxyl functional groups, which promotes the adhesion of Cr(III) to sorbents. This indicates that lignin plays the major role in the sorption of Cr(VI), and therefore explains the high biosorption efficiency

of CM. Besides lignocellulosic content, the surface morphology also influenced the sorption performance (Figure 1). Although S is composed of significantly higher lignin content than CG, it did not show greater sorption efficiency. This may have been due to the smooth surface of S although defined pores were observed, while CG possessed uneven surface and smaller pores, thus increasing the overall surface area and strengthening the adhesion between Cr ions and sorbent. Rough surface was also observed in CM, further explaining the high sorption performance. The surface of C consisted of observable pores, but the overall surface was sleek. In addition, protonation occured less significantly in C than in the other sorbents as the pH_{pzc} of C was 4.10, which resulted in low Cr(VI) sorption. The synergistic effect of high lignin content, high pHpzc and the rough surface morphology of CM was exemplified with high intrinsic sorption efficiency for Cr(VI).

Application of RSM

Determination of parameters range of operation. Before proceeding to RSM, a screening process was done to determine the region of interest and to select the suitable range of operation for the independent variables involved i.e. initial pH, CT, SR and SD. The effect of CT (15, 30, 60, 90, 180, 300, 480, 600, 840 and 1440 min) and SD (0.1, 0.25, 0.5, 0.75 and 1.0 g) were investigated in 50 mL of 200 mg/L Cr(VI) solution at pH 2 and RT. The respective % removal of Cr(VI) at different time intervals was 29.15%, 36.30%, 38.95%, 39.58%, 46.15%, 53.51%, 54.33%, 55.02%, 59.41% and 60.43%. The corresponding quantity SD range that was studied gave 30.58%, 50.30%, 62.62%, 79.89% and 84.96% of sorption. The ranges of 15-300 min and 0.1-1.0 g of SD were selected as rapid changes and the region of interest fall within this range. The range of initial pH was set at pH 1-5 because the sorption of Cr(VI) happens effectively at lower pH values (pH<3) (Saha et al., 2012). An SR with the range of 60-350 r/min was selected as higher SR increases the cost of operation, making it economically undesirable.

Model fitting. The 30 experimental runs of the four-factor three-level FCCD and their output responses (% removal) are shown in Table 3. The data were analysed through cubic, quadratic, two-factor interaction and linear models. A suitable model was selected based on a few important factors i) highest order polynomial where additional terms are significant, ii) not aliased, iii) insignificant lack-of-fit and iv) highest adjusted and predicted R-squared. A quadratic model was selected as it fulfilled all the aforementioned aspects (adjusted R^2=0.9635, predicted R^2=0.8819). The selected quadratic model was improved using backward elimination regression with alpha to exit equals to 0.1. Backward elimination bypassed terms with the highest p-value one by one until the next term satisfied the alpha criterion. SR was eliminated throughout the process as it showed insignificant effect and was not required to support the hierarchy of the model. Table 4 shows the analysis of variance (ANOVA) for the reduced quadratic model. The lowest and highest percentage removal was 15.90% and 74.63%, respectively. The biosorption of Cr(VI) was highly influenced by the initial pH, CT and SD ($p<0.0001$). Furthermore, the quadratic effects of pH and CT as well as the interactive effect of pH and SD also affected biosorption significantly ($p<0.0001$). The reduced quadratic model was statistically significant ($p<0.0001$) with a high R^2 (0.9788) and adjusted R^2 (0.9733). The predicted R^2 (0.9601) was in reasonable

agreement with the adjusted R^2 and had high adequate precision (48.649). This indicated that the model gave a good prediction on the response. Furthermore, the lack-of-fit test was also insignificant ($p>0.05$); this confirmed that the empirical relationship between the response and the variables involved can be sufficiently described through the following polynomial:

$$\% \text{ Removal} = 28.10 - 13.53x_1 + 0.16x_2 + 54.14x_4 - 8.80x_1 x_4 + 1.99x_1^2 - (3.75E\text{-}004)x_2^2$$

Table 3
Face-centred central composite design (FCCD) of four independent factors along with output responses

Standard	Run	Independent Variables				Percentage Removal (%)
		x_1	x_2	x_3	x_4	
14	1	5	15	350	1.00	20.65
5	2	1	15	350	0.10	21.65
6	3	5	15	350	0.10	17.20
9	4	1	15	60	1.00	65.13
13	5	1	15	350	1.00	66.46
2	6	5	15	60	0.10	15.90
10	7	5	15	60	1.00	20.25
19	8	3	15	205	0.55	23.95
1	9	1	15	60	0.10	20.35
25	10	3	157.5	205	0.55	34.80
17	11	1	157.5	205	0.55	62.70
30	12	3	157.5	205	0.55	37.55
28	13	3	157.5	205	0.55	33.40
23	14	3	157.5	205	0.10	21.75
21	15	3	157.5	60	0.55	38.00
26	16	3	157.5	205	0.55	38.55
18	17	5	157.5	205	0.55	30.60
29	18	3	157.5	205	0.55	37.95
24	19	3	157.5	205	1.00	50.96
22	20	3	157.5	305	0.55	38.60
27	21	3	157.5	205	0.55	36.55
8	22	5	300	350	0.10	25.40
16	23	5	300	350	1.00	37.95
4	24	5	300	60	0.10	23.90
15	25	1	300	350	1.00	74.63
11	26	1	300	60	1.00	73.07
3	27	1	300	60	0.10	36.35
20	28	3	300	205	0.55	38.15
12	29	5	300	60	1.00	37.85
7	30	1	300	350	0.10	39.85

x_1: initial pH; x_2: CT (min); x_3: SR (r/min); x_4: SD (g)

Table 4
Analysis of variance (ANOVA) for reduced quadratic model

Source	SS	df	MS	F Value	Prob > F	Significance
Model	7744.83	6	1290.80	177.28	<0.0001	*
x_1	2951.17	1	2951.17	405.32	<0.0001	*
x_2	742.67	1	742.67	102.00	<0.0001	*
x_4	2802.26	1	2802.26	384.87	<0.0001	*
x_1x_4	1004.57	1	1004.57	137.97	<0.0001	*
x_1^2	219.32	1	219.32	30.12	<0.0001	*
x_2^2	200.03	1	200.03	27.47	<0.0001	*
Residual	167.46	23	7.28			
Lack of Fit	147.56	18	8.20	2.06	0.2174	NS
Pure Error	19.90	5	3.98			
Cor Total	7912.29	29				
Standard Deviation	2.70		R-squared		0.9788	
Mean	37.34		Adj R-squared		0.9733	
C.V. %	7.23		Pred R-squared		0.9601	
PRESS	315.34		Adeq precision		48.649	

x_1: initial pH; x_2: CT (min); x_4: SD (g); SS: sum of squares; df: degree of freedom; MS: mean square; NS: not significant; * indicates significant

Effect of single factor. The perturbation graph shows and compares the effect of each factor on the percentage removal of Cr(VI) at the middle level in the design space (Figure 3a). Initial pH of the solution affected the biosorption most significantly, as the percentage removal increased from 30.60% to 62.70% when the pH decreased from 5 to 1 while the other factors remained constant. The initial pH of the solution had a high influence on biosorption because the pH not only affected the surface characteristic of the sorbent, but also changed the speciation of chromium ions. At pH<6, the dominant Cr(VI) species is $Cr_2O_7^{2-}$ and $HCrO_4^-$ anion (Rai et al., 1989). Meanwhile, the surface of the sorbent was protonated at pH<pH_{pzc} (pH_{pzc}=7.30), causing the surface to become positively charged. The dominant anionic species $HCrO_4$- and $Cr_2O_7^{2-}$ were therefore highly attracted to the positively-charged surface of the sorbent at low pH. As the pH increased, the degree of protonation decreased, making the surface less positive, which in turn reduced the percentage removal. Initial pH of the solution had little effect on biosorption at pH>4.

The SD affected percentage removal to the same extent as that of the initial pH of the solution. The percentage removal of Cr(VI) increased linear from 21.75% to 50.96% when the SD increased 10 times from 0.1 g, while the other factors remained constant. This is because there were more available sorption sites for the metal ions, creating a less competitive

environment as the SD increased; thus, more metal ions were successfully attached to the sorbent. The percentage removal had not reached saturation in the studied SD range.

Followed by initial pH of the solution and SD, the percentage removal of Cr(VI) was significantly influenced by CT. Biosorption happened rapidly from 15 min to around 240 min, where the percentage removal increased from 23.95% to 38.29% and reached a plateau around 240 min onwards and recorded 38.15% at 300 min. CT did not have a significant interactive effect with both solution pH and SD. Thus, the same trend was observed at different initial pH and SD ranges where biosorption was completed at around 240min.

The SR was not included in the reduced quadratic model as it did not have a significant effect on the biosorption. Although SR was expected to increase the kinetic energy of metal ions and enhance diffusion of metal ions through the sorbent, the percentage removal had a negligible effect when the SR increased from 60 to 350 r/min in the whole range of initial pH and SD studied. SR also did not accelerate the sorption process. This indicated that vigorous agitation is not required to enhance the biosorption, but minimum agitation which provides enough mixing of the mixture was adequate. This is good as increasing agitation speed would definitely increase the cost of operation.

Interaction between factors. The interaction between the solution's initial pH and SD was highly significant ($p<0001$). Interaction plots showed the interaction between these two variables at 157.5 min and 60 r/min (Figure 3b). The combined effect of low pH and high SD accounted for the highest percentage removal of Cr(VI) (78.31% removal at pH 1 and 1.0 g). However, the synergistic effect was greatly reduced as the pH increased from 1 to 5. At pH 1 and 3, the percentage removal increased from 37.50% to 78.31% and 21.75% to 50.96%, respectively when the SD was raised from 0.1 g to 1.0 g. The sorption efficiency was doubled at both pH 1 and 3 when SD was 10 times higher. However, the increment in sorption efficiency caused by higher SD dropped dramatically at pH=5. Only 27.74% removal was observed in 0.1 g sorbent and this increased slightly to 36.85% in 1.0 g of sorbent. This phenomenon occurred because protonation happened at low pH, causing the surface of the sorbent to be positively charged, aiding the sorption of anionic species of Cr(VI), i.e. $HCrO_4^-$ and $Cr_2O_7^{2-}$. Therefore, when the SD increased at low pH, all the active sites were adequately protonated; there were more functional positively-charged active sites available for sorption. However, when the pH shifted towards pH 5, the degree of protonation slowed down, hence, even when the SD was higher, the surface of the sorbent was not available for metal ions as they were not sufficiently protonated. The non-protonated active sites were unable to adsorb the anionic species due to the repulsive force between like charges.

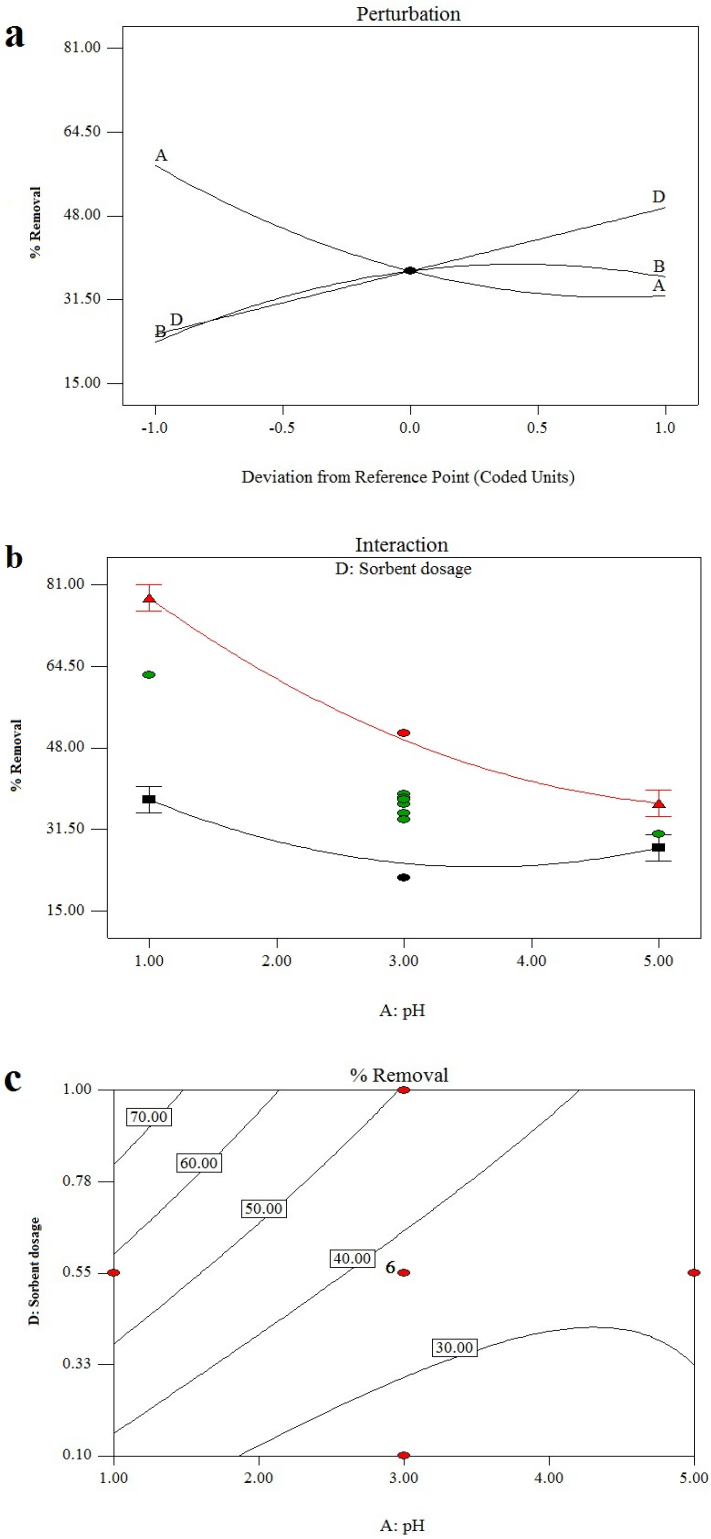

Figure 3. (a) Perturbation graph of the effect of single variables (b) Interactive effect of pH and SD and (c) Contour plot shows the optimum condition for the biosorption of Cr(VI) at the middle level in the design space

Response optimisation and validation experiment. The contour plot and numerical optimisation function in Design Expert 7.0.0 software can be used to predict the optimum condition. The optimum operational range was roughly estimated through the contour plot and the exact optimum range was determined through numerical optimisation function. The goal (maximise, minimise, target to or in range) was set for each variable and output response, and a list of solutions with desirability were generated. In the optimisation process, SR was minimised (60 r/min) since this variable had little effect on biosorption. Through numerical optimisation and the analysis of the contour plot generated as shown in Figure 3c, the maximum range of percentage removal (≥70%) occurred at the following optimum range: initial pH 1-1.56, 0.79-1 g of sorbent and 57-300 min CT. The specific optimum operating condition for maximum removal was then determined by setting the goal for initial pH, SD and CT within the optimum range as stated above. The predicted maximum percentage removal (78.43%) could be achieved at pH 1.04, 212.37 min, 60 r/min and 0.99 g of sorbent in 50 mL of 200 mg/L metal ion solution with desirability of 1. In order to validate the quadratic model, the solutions suggested by software were carried out experimentally (Table 5). In all three solutions, the goal for all the variables was set within the experimental range except when the SR was minimised. The output response for solution 1 and 2 was maximised, while it was set within the range of 50%-74.63% in solution 3. The experimental results were close to the predicted value with residual less than 4.65% in all the three solutions tested. A chi-square test (X^2) was carried out to determine the goodness-of-fit between the experimental and predicted values at the degree of freedom = 2. The results were accepted as significant when X^2 was more than the critical value at the 0.05 level of significance (5.991). The chi-square (0.47) obtained was smaller than the critical value (5.991), which indicated that there was no significant difference between the experimental and predicted values ($p>0.05$). In other words, the model was able to give a valid prediction.

Table 5
Response optimisation and model validation

Solution	x_1	x_2	x_3	x_4	D	Percentage Removal (%)		R	X^2
						Est.	Exp.		
1	1.04	157.97	60	0.99	1.000	77.21	79.00	1.79	0.47
2	1.15	212.11	60	0.96	1.000	75.25	75.07	0.18	
3	1.07	162.19	60	0.40	1.000	50.49	55.14	4.65	

x_1: initial pH; x_2: CT (min); x_3: SR (r/min); x_4: SD (g); D: desirability; Est.: estimated; Exp.: experimental; R: residual; X^2: Chi-square

Biosorption Kinetics

The pseudo-first-order equation is based on Lagergren's first-order equation (Lagergren, 1898), in which metal ions are assumed to bind to only one binding site and the adsorption rate is

proportional to the number of available sorption sites as expressed in Equation [5]. The integral and linear form is shown in Equation [6].

$$\frac{dq_t}{dt} = k_1(q_e - q_t) \quad [5]$$

$$log(q_e - q_t) = log\, q_e - \frac{k_1}{2.303}t \quad [6]$$

where t is the CT (min), q_e and q_t are the metal uptake of sorbent at equilibrium and at time t (mg/g), respectively, and k_1 is the pseudo-first-order rate constant (min^{-1}). Estimated q_e and k_1 were determined from the slope and intercept of the graph of log (q_e - q_t) against t (Figure 4a).

The pseudo-second-order reaction, in contrast, assumes metal ions are adsorbed to two binding sites (Ahmady-Asbchin et al., 2015). The relationship between the driving force, (q_e - q_t) and the adsorption rate is expressed in Equation [7], and its integral and linear form is shown in Equation [8].

$$\frac{dq_t}{dt} = k_2(q_e - q_t)^2 \quad [7]$$

$$\frac{t}{q_t} = \frac{1}{q_e{}^2 k_2} + \frac{1}{q_e}t \quad [8]$$

where k_2 is the pseudo-second-order rate constant (g mg^{-1} min^{-1}). The slope and intercept of the straight line from the plot of t/q_t against t (Figure 4b) were used to obtain k_2 and estimated q_e.

The parameters of both the pseudo-first-order and pseudo-second-order models are shown in Table 6. The biosorption data were best fitted in the pseudo-second-order with R^2=0.9964 rather than the pseudo-first-order, in which the R^2 was only 0.9427. Besides that, the good agreement of the experimental q_e (12.09 mg/g) to the estimated q_e (12.00 mg/g) from the pseudo-second-order further supported the conclusion that the sorption process is best described by pseudo-second-order model.

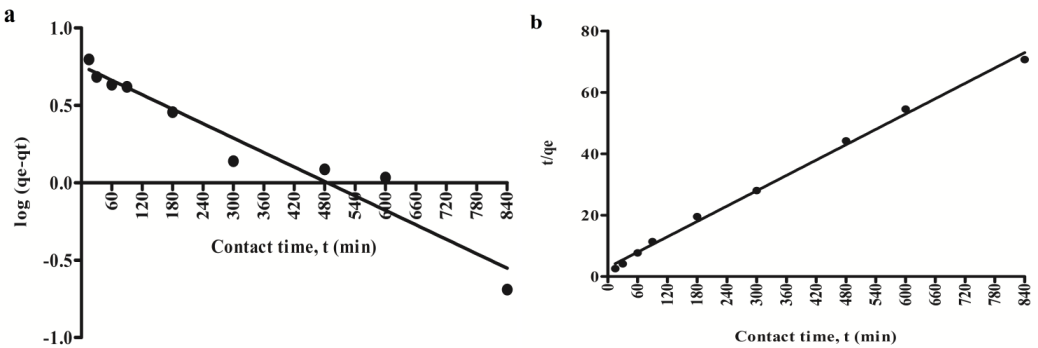

Figure 4. (a) Pseudo-first-order and (b) pseudo-second-order model for biosorption of Cr(VI) by CM (MC: 200 mg/L, pH: 2, SD: 0.5 g, SR: 350 r/min, temperature: 25°C)

Table 6
Kinetic parameters for the biosorption of Cr(VI) by CM

Kinetic models	Parameters	Value	R-squared
Pseudo-first-order	q_e (mg/g)	5.70	0.9427
	k_1 (min^{-1})	0.0037	
Pseudo-second-order	q_e (mg/g)	12.00	0.9964
	k_2(g mg^{-1} min^{-1})	0.0023	
	h (mg g^{-1} min^{-1})	0.3386	
Experimental	q_e (mg/g)	12.0860	NA

NA: not available

Biosorption Isotherm

Adsorption isotherm describes the equilibrium relationship between sorbate and sorbent. It also provides a better understanding of the sorption capacity and pathway involved. Langmuir and Freundlich isotherms are two widely used models in liquid-solid adsorption system.

Langmuir isotherm (Langmuir, 1916) presumes that the sorbent has a homogenous surface with a finite number of sorption sites that possess constant sorption affinity for the sorbate. It suggests monolayer adsorption, in which there is no interaction between adjacent adsorbed molecules. The Langmuir model and its linear form are expressed in Equation [9] and [10], respectively.

$$q_e = \frac{q_m b C_e}{1 + b C_e} \quad [9]$$

$$\frac{C_e}{q_e} = \frac{1}{b q_m} + \frac{1}{q_m} C_e \quad [10]$$

where q_e and C_e are the metal uptake of sorbent (mg/g) and final MC at equilibrium, respectively; q_m is the maximum monolayer sorption capacity (mg/g) and b is the Langmuir equilibrium constant related to sorption affinity (L/mg) obtained from the plot of C_e/q_e against C_e (Figure 5a).

The b value can be used to obtain the dimensionless separation factor through Equation [11]

$$R_L = \frac{1}{1 + b C_o} \quad [11]$$

where R_L is the dimensionless separation factor, b is the Langmuir constant and C_0 is the initial MC. R_L>1 indicates unfavourable sorption, 0<R_L<1 indicates favourable sorption, R_L=0 indicates irreversible sorption and R_L=1 is linear sorption.

The Freundlich isotherm (Freundlich, 1906), in contrast, is used to describe sorption on heterogeneous surfaces with varying sorption affinity. This model can be applied in a multilayer

sorption system, and it assumes that the sorption affinity decreases when a sorption site is being occupied (Vijayaraghavan et al., 2006). The relationship is expressed in Equation [12]

$$q_e = k_f C_e^{\frac{1}{n}} \quad [12]$$

The linear Freundlich model is shown in Equation [13]

$$log\ q_e = log\ k_f + \frac{1}{n}\ log\ C_e \quad [13]$$

where k_f is the Freundlich constant related to multilayer adsorption capacity and n is the Freundlich constant related to adsorption intensity. The slope and intercept of the graph of $log\ q_e$ against $log\ C_e$ (Figure 5b) were used to determine k_f and n, respectively.

The isothermal parameters of both models at different temperatures (298 K, 308 K and 318 K) are shown in Table 7. The q_m and k_f values increased with temperature. This may be due to the rise in kinetic energy, which improves the collision frequency between metal ions and the sorbent (Khan et al., 2012). In addition, the heat dilates the pores and slightly opens up the structure of the sorbents, which eases intraparticle diffusion within the pores (Meena et al., 2008). The n value obtained from the Freundlich model lay in the range of 1-10 (2.2753-2.6048), while the separation factor, R_L, was in the range of)-1 (0.03-0.45); both observations suggested favourable adsorption (Slejko, 1985; Treybal, 1980) in the whole range of the initial MC and temperature studied. Based on the correlated coefficient, the equilibrium relationship was better described by the Langmuir models (R^2>0.9882) compared to the Freundlich models (R^2<0.9523).

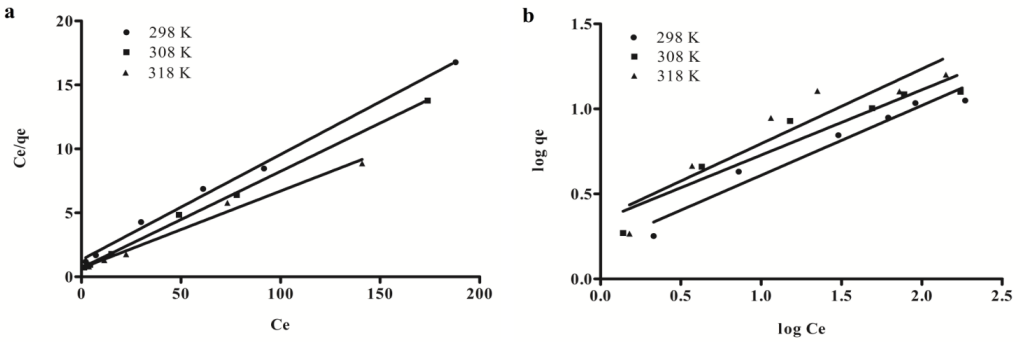

Figure 5. (a) Langmuir and (b) Freundlich isotherm for biosorption of Cr(VI) by CM at different temperatures (pH: 2, SD: 0.5 g, SR: 350 r/min, CT: 480 min)

Table 7
Isotherm parameters for the Biosorption of Cr(VI) by CM at different temperatures

Isotherm Models	Parameters	Value		
		298 K	308 K	318 K
Langmuir	q_m(mg/g)	12.14	13.26	16.60
	b (L/mg)	0.0621	0.1070	0.0888
	R^2	0.9950	0.9979	0.9882
	R_L	0.05-0.45	0.03-0.32	0.04-0.36
Freundlich	k_f[(mg/g)(L/mg)$^{1/n}$]	1.58	2.21	2.27
	n (g/L)	2.4349	2.6048	2.2753
	R^2	0.9523	0.9034	0.8622

Thermodynamic Studies

Thermodynamic parameters i.e. Gibb's free energy change (ΔG), enthalpy energy change (ΔH) and entropy energy change (ΔS) are related to each other in Equation [14] and ΔG is defined in Equation [15].

$$\Delta G = \Delta H - T\Delta S \quad [14]$$

$$\Delta G = -RT ln\, K \quad [15]$$

$$K = \left(\frac{C_s}{C_e}\right) \quad [16]$$

Equation [14] and [15] are combined and to yield the Van't Hoff equation as shown in Equation [17]

$$ln\, K = \left(\frac{\Delta H}{R}\right) - \left(\frac{\Delta S}{RT}\right) \quad [17]$$

where R is the universal gas constant (8.314 $J^{-1}mol\text{-}1K^{-1}$), T is the absolute temperature (K), C_s and C_e are the MC on the sorbent and the final MC remains in the solution at equilibrium (mg/g), respectively. ΔH and ΔS can be obtained from the Van't Hoff plot of $ln\, K$ against $1/T$.

The thermodynamic parameters are shown in Table 8. The negative value of ΔG indicated that the sorption process was spontaneous. ΔG was more negative in the lower initial MC and became less negative as the concentration increased, which revealed that the sorption process was more spontaneous in lower initial MC. This can be attributed to high availability of free sorption sites in relatively low MC solution. When the initial MC increased to 300 mg/L, the biosorption became unfavourable (ΔG became positive at 298 K and 308 K) as the binding sites of the sorbent had reached saturation. ΔG also reflected that the spontaneity was greater when the temperature increased. The positive value of ΔH indicated the biosorption process was endothermic. The positive value of ΔS indicated the increase in randomness of the sorbent-solution interface during the biosorption process (Ahmady-Asbchin et al., 2015).

Table 8
Thermodynamic parameters for the Biosorption of Cr(VI) by CM

Initial MC, C0 (mg/L)	Temperature (K)	ΔG (KJ mol^{-1})	ΔH (KJ mol^{-1})	ΔS (KJ mol^{-1} K^{-1})
20	298	-5.288	14.377	0.0668
	308	-6.670		
	318	-6.591		
50	298	-4.418	29.054	0.1129
	308	-6.072		
	318	-6.652		
100	298	-2.103	47.081	0.1657
	308	-4.417		
	318	-5.389		
150	298	-0.929	53.408	0.1814
	308	-1.856		
	318	-4.596		
200	298	-0.412	15.102	0.0523
	308	-1.146		
	318	-1.449		
300	298	1.280	24.966	0.0791
	308	0.823		
	318	-0.318		

Desorption and Regeneration

The amount of Cr(VI) desorbed after 30 min, 5 h and 24 h CT was 14.50 mg/L, 34.03 mg/L and 67.51 mg/L, respectively (Figure 6[a]). Since the concentration of NaOH could not be increased further as it would have destroyed the morphology of the sorbent (Wang et al., 2013), 24 h CT was chosen to desorb Cr(VI) in the regeneration study as it showed a higher desorption. Desorption efficiency in the first, second and third desorption cycle was 35.66%, 46.0% and 54.62%, respectively (Figure 6b). The adsorption efficiency decreased from 76.35% in the first cycle to 52.51% in the third cycle, suggesting that some Cr(VI) that had formed a stronger interaction with the binding sites were more difficult to desorb and they remained attached to the binding site; thus, fewer binding sites were available for subsequent sorption.

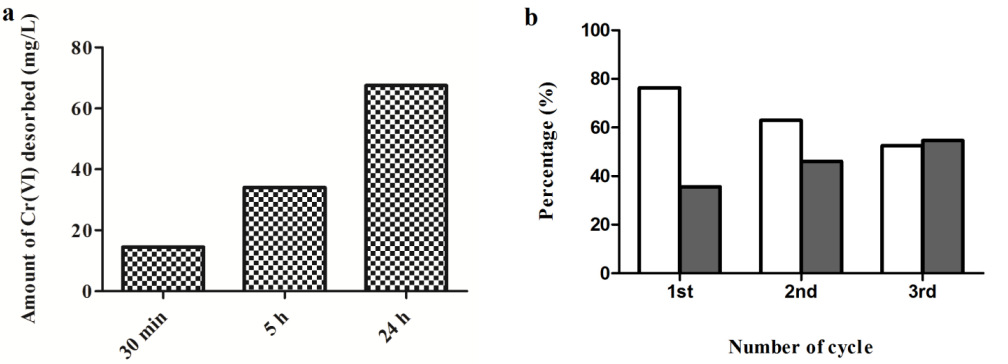

Figure 6. (a) Desorption of Cr(VI) using 50 mL of 0.1 M NaOH at different CT and (b) the adsorption (no filled column) and desorption (filled column) efficiency of CM loaded with Cr(VI)

Sorption Pathway

During rapid sorption in the first 30 min, ΔG in the range of -20 to 0 KJ mol^{-1} and $\Delta H<40$ KJ mol^{-1} in majority conditions indicated that physisorption was involved (Poulopoulos & Inglezakis, 2006; Weil, 1981). However, the endothermic nature observed wherein the q_m increased with temperature and a long equilibrium time (major sorption completed at 300 min) suggested that chemisorption also played a role in the sorption (Tran et al., 2016). Possible desorption confirmed that physisorption on the surface of the sorbents was involved. Nevertheless, low desorption efficiency and the significant drop in adsorption efficiency with the number of adsorption-desorption cycles confirmed that stronger chemical bonds were involved in addition to the physical bonding.

CONCLUSION

Biosorption of Cr(VI) using fresh CM without structural modification was examined in this study. Results showed that CM possessed significantly higher sorption efficiency compared to C, S and CG due to its fibrous, ligneous nature and rough surface morphology. The solution's initial pH, CT and SD significantly affected biosorption, while SR had negligible effect on biosorption. The combined effect of high SD and low pH was responsible for the highest sorption efficiency. The initial pH of the solution 1-1.56, 0.79-1 g of sorbent and 57-300 min of CT were able to remove ≥70% Cr(VI). Kinetic studies confirmed that the biosorption of Cr(VI) obeyed the pseudo-second-order model (R^2=0.9964). The equilibrium relationship between the sorbent and metal ions was well described by the Langmuir isotherm model (R^2>9882). The maximum monolayer sorption capacity of the CM was 12.14 mg/g at 298 K. Thermodynamic studies confirmed that the sorption process was spontaneous and endothermic. The recovery of Cr(VI) was possible and the CM was able to be reused at least three times with adsorption efficiency remaining >50%. Based on the combined observation of the kinetic, isotherm, thermodynamic and regeneration studies, it is suggested that the sorption of Cr(VI) involved both the physisorption and chemisorption processes. Intrinsically, the advantageous properties of CM (plentiful, low-cost, regenerable, fibrous, ligneous, rough surface morphology and

significantly high sorption for Cr[VI]) enabled it to be employed with minimum requirement of subsequent chemicals or thermochemical pre-treatment to enhance its sorption efficiency. Therefore, CM is a potential low-cost and an environmentally-friendly biosorbent for Cr(VI) removal.

REFERENCES

Ahmady-Asbchin, S., Safari, M., & Varposhti, M. (2015). Biosorption optimization of Cr(VI) using response surface methodology and thermodynamics modeling onto *Azolla filiculoides*. *Separation Science and Technology, 50*(4), 554–563.

Al-Rub, F., Kandah, M., & Al-Dabaybeh, N. (2002). Nickel removal from aqueous solutions using sheep manure wastes. *Engineering in Life Sciences, 2*(4), 111.

Bailey, S. E., Olin, T. J., Bricka, R. M., & Adrian, D. D. (1999). A review of potentially low-cost sorbents for heavy metals. *Water Research, 33*(11), 2469–2479.

Barakat, M. (2011). New trends in removing heavy metals from industrial wastewater. *Arabian Journal of Chemistry, 4*(4), 361–377.

Boehm, H. (1966). Chemical identification of surface groups. *Advances in catalysis* (pp. 179–274). New York: Academic Press.

Chen, S., Liao, W., Liu, C., Wen, Z., Kincaid, R., Harrison, J., Elliott, D., … & Stevens, D., (2003). *Value-added chemicals from animal manure-final technical report-contract DE-AC06-76RL0 1830*. US Department of Energy (USA).

Chowdhury, M., Mostafa, M., Biswas, T., Mandal, A., & Saha, A. (2015). Characterization of the effluents from leather processing industries. *Environmental Processes, 2*(1), 173–187. doi: 10.1007/s40710-015-0065-7

Dupont, L., Bouanda, J., Ghanbaja, J., Dumonceau, J., & Aplincourt, M. (2004). Use of analytical microscopy to analyze the speciation of copper and chromium ions onto a low-cost biomaterial. *Journal of Colloid and Interface Science, 279*(2), 418–424.

Dupont, L., & Guillon, E. (2003). Removal of hexavalent chromium with a lignocellulosic substrate extracted from wheat bran. *Environmental Science and Technology, 37*(18), 4235–4241.

EPA. (2001). *Method 1684 total, fixed, and volatile solids in water, solids, and biosolids* (pp. 1–13). US Environmental Protection Agency.

FAOSTAT. (2013). *Live animals' production*. Retrieved July 25, 2015, from http://faostat3.fao.org/download/Q/QA/E

Freundlich, H. (1906). Over the adsorption in solution. *Journal of Physical Chemistry, 57*(385), e470.

Fu, F., & Wang, Q. (2011). Removal of heavy metal ions from wastewaters: A review. *Journal of Environmental Management, 92*(3), 407–418.

Garg, U., Kaur, M., Garg, V., & Sud, D. (2008). Removal of nickel (II) from aqueous solution by adsorption on agricultural waste biomass using a response surface methodological approach. *Bioresource Technology, 99*(5), 1325–1331.

Gupta, V., Ali, I., Saleh, T., Nayak, A., & Agarwal, S. (2012). Chemical treatment technologies for waste-water recycling – An overview. *RSC Advances, 2*(16), 6380-6388.

Harman, G., Patrick, R., & Spittler, T. (2007). Removal of heavy metals from polluted waters using lignocellulosic agricultural waste products. *Industrial Biotechnology, 3*(4), 366–374.

Hofmann, N., & Beaulieu, M. (2006). *A geographical profile of manure production in Canada, 2001*. Statistics Canada, Agriculture Division.

IARC. (2012). Chromium (VI) compounds. IARC Monographs, 100 C, 147–167.

Jordão, C., Fernandes, R., de Lima Ribeiro, K., de Barros, P., Fontes, M., & de Paula Souza, F. (2010). A study on Al(III) and Fe(II) ions sorption by cattle manure vermicompost. *Water, Air and Soil Pollution, 210*(1–4), 51–61.

Jordão, C., Pereira, W., Carari, D., Fernandes, R., De Almeida, R., & Fontes, M. (2011). Adsorption from brazilian soils of Cu(II) and Cd(II) using cattle manure vermicompost. *International Journal of Environmental Studies, 68*(5), 719–736.

Khan, M., Ngabura, M., Choong, T., Masood, H., & Chuah, L. (2012). Biosorption and desorption of nickel on oil cake: Batch and column studies. *Bioresource Technology, 103*(1), 35–42.

Lagergren, S. (1898). About the theory of so-called adsorption of soluble substances. *Kungliga Svenska Vetenskapsakademies Handlingar, 24*(4), 1–39.

Langmuir, I. (1916). The constitution and fundamental properties of solids and liquids: Part I, solids. *Journal of the American Chemical Society, 38*(11), 2221–2295.

Lima, I., & Marshall, W. (2005a). Adsorption of selected environmentally important metals by poultry manure-based granular activated carbons. *Journal of Chemical Technology and Biotechnology, 80*(9), 1054–1061.

Lima, I., & Marshall, W. (2005b). Utilization of turkey manure as granular activated carbon: Physical, chemical and adsorptive properties. *Waste Management, 25*(7), 726–732.

Masood, F., & Malik, A. (2011). Biosorption of metal ions from aqueous solution and tannery effluent by Bacillus sp. FM1. *Journal of Environmental Science and Health, Part A, 46*(14), 1667–1674.

Meena, A., Kadirvelu, K., Mishra, G., Rajagopal, C., & Nagar, P. (2008). Adsorptive removal of heavy metals from aqueous solution by treated sawdust (*Acacia arabica*). *Journal of Hazardous Materials, 150*(3), 604–611.

Meng, J., Feng, X., Dai, Z., Liu, X., Wu, J., & Xu, J. (2014). Adsorption characteristics of Cu(II) from aqueous solution onto biochar derived from swine manure. *Environmental Science and Pollution Research, 21*(11), 7035–7046.

Miretzky, P., & Cirelli, A. (2010). Cr(VI) and Cr(III) removal from aqueous solution by raw and modified lignocellulosic materials: A review. *Journal of Hazardous Materials, 180*(1), 1–19.

Ngah, W., & Hanafiah, M. (2008). Removal of heavy metal ions from wastewater by chemically modified plant wastes as adsorbents: A review. *Bioresource Technology, 99*(10), 3935–3948.

Poulopoulos, S. G., & Inglezakis, V. J. (2006). *Adsorption, ion exchange and catalysis: Design of operations and environmental applications.* The Netherlands: Elsevier.

Rai, D., Eary, L., & Zachara, J. (1989). Environmental chemistry of chromium. *Science of the Total Environment, 86*(1–2), 15–23.

Saha, P., Dey, A., & Marik, P. (2012). Batch removal of chromium (VI) from aqueous solutions using wheat shell as adsorbent: Process optimization using response surface methodology. *Desalination and Water Treatment, 39*(1–3), 95–102.

Shazili, N., Yunus, K., Ahmad, A., Abdullah, N., & Rashid, M. (2006). Heavy metal pollution status in the Malaysian aquatic environment. *Aquatic Ecosystem Health and Management, 9*(2), 137–145.

Slejko, F. L. (1985). *Adsorption technology: A step-by-step approach to process evaluation and application*. Dekker New York: Basel.

Tran, H. N., You, S. J., & Chao, H. P. (2016). Thermodynamic parameters of cadmium adsorption onto orange peel calculated from various methods: A comparison study. J*ournal of Environmental Chemical Engineering, 4*(3), 2671–2682.

Treybal, R. (1980). *Mass transfer operations, 1980* (3rd Ed.). New York: Mc-Graw Hill Book Company.

Uchimiya, M., Lima, I., Thomas, K., Chang, S., Wartelle, L., & Rodgers, J. (2010). Immobilization of heavy metal ions (Cu(II), Cd(II), Ni(II), and Pb(II)) by broiler litter-derived biochars in water and soil. *Journal of Agricultural and Food Chemistry, 5*8(9), 5538–5544.

Vijayaraghavan, K., Padmesh, T., Palanivelu, K., & Velan, M. (2006). Biosorption of nickel (II) ions onto *Sargassum wightii*: Application of two-parameter and three-parameter isotherm models. *Journal of Hazardous Materials, 133*(1), 304–308.

Vikramjit, S., Chhotu, R., & Ashok, K. (2016). Physico-Chemical Characterization of Electroplating Industrial Effluents of Chandigarh and Haryana Region. *Journal of Civil and Environmental Engineering, 6*(4), 1-6.

Wang, J., Pan, K., He, Q., & Cao, B. (2013). Polyacrylonitrile/polypyrrole core/shell nanofiber mat for the removal of hexavalent chromium from aqueous solution. *Journal of Hazardous Materials, 244*, 121–129.

Water, U. N. (2009). *The United Nations world water development report 3 –Water in a changing world.* Paris: United Nations Educational Scientific and Cultural Organization.

Weil, K. G. (1981). MJ Jaycock, GD Parfitt: Chemistry of Interfaces. Ellis Horwood Limited Publishers, Chichester 1981. 279 Seiten, Preis:£ 27, 50. *Berichte der Bunsengesellschaft für physikalische Chemie, 85*(9), 718–718.

Zaini, M., Okayama, R., & Machida, M. (2009). Adsorption of aqueous metal ions on cattle-manure-compost based activated carbons. *Journal of Hazardous Materials, 170*(2), 1119–1124.